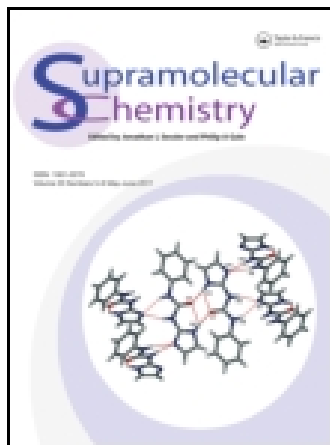


This article was downloaded by: [UNAM Ciudad Universitaria]

On: 27 December 2014, At: 16:34

Publisher: Taylor & Francis

Informa Ltd Registered in England and Wales Registered Number: 1072954 Registered office: Mortimer House, 37-41 Mortimer Street, London W1T 3JH, UK



Supramolecular Chemistry

Publication details, including instructions for authors and subscription information:

<http://www.tandfonline.com/loi/gsch20>

Pre-organisation or a hydrogen bonding mismatch: silver(I) diamide ligand coordination polymers versus discrete metallo-macrocyclic assemblies

Maisara Abdul-Kadir ^a, Philip R. Clements ^a, Lyall R. Hanton ^b, Courtney A. Hollis ^a & Christopher J. Sumbly ^a

^a School of Chemistry and Physics, The University of Adelaide, Adelaide, Australia

^b Department of Chemistry, University of Otago, Dunedin, New Zealand

Published online: 04 Jul 2012.

To cite this article: Maisara Abdul-Kadir, Philip R. Clements, Lyall R. Hanton, Courtney A. Hollis & Christopher J. Sumbly (2012) Pre-organisation or a hydrogen bonding mismatch: silver(I) diamide ligand coordination polymers versus discrete metallo-macrocyclic assemblies, *Supramolecular Chemistry*, 24:8, 627-640, DOI: [10.1080/10610278.2012.699052](https://doi.org/10.1080/10610278.2012.699052)

To link to this article: <http://dx.doi.org/10.1080/10610278.2012.699052>

PLEASE SCROLL DOWN FOR ARTICLE

Taylor & Francis makes every effort to ensure the accuracy of all the information (the "Content") contained in the publications on our platform. However, Taylor & Francis, our agents, and our licensors make no representations or warranties whatsoever as to the accuracy, completeness, or suitability for any purpose of the Content. Any opinions and views expressed in this publication are the opinions and views of the authors, and are not the views of or endorsed by Taylor & Francis. The accuracy of the Content should not be relied upon and should be independently verified with primary sources of information. Taylor and Francis shall not be liable for any losses, actions, claims, proceedings, demands, costs, expenses, damages, and other liabilities whatsoever or howsoever caused arising directly or indirectly in connection with, in relation to or arising out of the use of the Content.

This article may be used for research, teaching, and private study purposes. Any substantial or systematic reproduction, redistribution, reselling, loan, sub-licensing, systematic supply, or distribution in any form to anyone is expressly forbidden. Terms & Conditions of access and use can be found at <http://www.tandfonline.com/page/terms-and-conditions>

Pre-organisation or a hydrogen bonding mismatch: silver(I) diamide ligand coordination polymers versus discrete metallo-macrocylic assemblies

Maisara Abdul-Kadir^{a1}, Philip R. Clements^a, Lyall R. Hanton^b, Courtney A. Hollis^a and Christopher J. Sumbly^{a*}

^aSchool of Chemistry and Physics, The University of Adelaide, Adelaide, Australia; ^bDepartment of Chemistry, University of Otago, Dunedin, New Zealand

(Received 11 April 2012; final version received 10 May 2012)

The investigation of novel motifs to selectively complex anions is an area of considerable importance due to the significant environmental, biological and medicinal roles of anions. The synthesis of discrete metallo-macrocylic compounds or coordination polymers displaying anion-binding pockets can generate specific anion receptors from relatively simple components. Here, we examine the self-assembly of a series of flexible diamide compounds **L1**–**L5** with silver(I) metal salts. A new diamide ligand, 2,6-[*N,N'*-bis(di-(pyridin-2-yl)methyl)pyridine]-2,6-dicarboxamide (**L5**), with two chelating di-2-pyridylmethyl donor groups, was also prepared. Compounds **L1**–**L3**, lacking the pre-organising effect of a central 2,6-pyridine dicarboxamide core, form 1D coordination polymers {[Ag(**L1**)(CH₃CN)](PF₆)}_n (**6**), {[Ag(**L2**)](NO₃)(H₂O)}_n (**7**) and {[AgNO₃(**L3**)](CH₃OH)}_n (**9**) which in turn form 2D and 3D hydrogen-bonded networks through orthogonal hydrogen bonding. In one instance, **L2** gives rise to a dinuclear metallo-macrocycle in the solid state, [Ag₂(CF₃CO₂)₂(**L2**)₂][Ag₂(μ₂-CF₃CO₂)₂(**L2**)₂] (**8**). Both diamide ligands **L4** and **L5** form dinuclear metallo-macrocylics, [Ag₂(NO₃)₂(**L4**)₂] (**10**) and [Ag₂(**L5**)₂](NO₃)₂·2CH₃OH·2H₂O (**11**), in solution and in the solid state. Where possible, all compounds were investigated in solution and their solid-state structures were determined using X-ray crystallography. This enabled the effect of competing supramolecular synthons, covalent M–L bonding and hydrogen bonding, to be examined by comparing the solution and solid-state behaviour of each metal–ligand combination.

Keywords: metallo-supramolecular chemistry; coordination polymers; orthogonal interactions

1. Introduction

The development of novel metallo-supramolecular species with useful inclusion behaviour for neutral, cationic and anionic guests has been a focus of much research effort (1–6). These materials have been studied, for example, from the perspective of exploring the self-assembly of such compounds (2), to develop receptors (3, 5), to stabilise reactive intermediates or products, and for investigating catalysis within the closed environment of polyhedral assemblies (3, 4, 6). A related field of the study of anion binding has undergone a similar, rapid development (7–12). This birth of anion coordination chemistry (13) stems from the significant impact that anions have on environmental, biological and medicinal settings. Strategies to selectively complex anions require the synthesis of hosts utilising one or more of a toolbox of interactions (11), including hydrogen bond donor groups (10, 12), π-acidic heteroarene scaffolds (14–17), cationic groups for electrostatic interactions (11, 18) and Lewis acidic moieties (11).

The investigation of metallo-supramolecular assemblies (5, 19–22) and coordination polymers (23–25) as anion receptors and for anion separation or sequestration has also received attention. In the context of developing such systems for anion inclusion, the use of a metallo-supramolecular

species to bind anions can provide a number of advantages over neutral organic receptors (5, 20–22). Firstly, the anion binding and encapsulating aspects of a self-assembled system can be readily explored by combining a number of relatively simple organic ligands, which display moieties capable of interacting with anions, with different metal ions; the structural complexity required to bind an anion of interest is controlled by the choice of metal ion (26) (Figure 1(a)). Altering the affinity for a particular anion could be achieved by substituting in a different, but structurally similar, ligand (Figure 1(b)) or by changing the metal ion (26). Furthermore, labile transition metal centres might allow such receptors to respond to external stimuli, while the correct choice of metal centre could facilitate detection as a consequence of optical or electrochemical responses to binding (5).

The incorporation into metallo-supramolecular species and coordination polymers of ligands containing hydrogen bond donor groups has been explored (5, 27–31). In particular, transition metal complexes with pendant hydrogen bond donor groups have been investigated (5, 32, 33), and metallo-supramolecular assemblies with internal hydrogen bonding domains have also been reported (20, 21, 26, 34–38). Such self-assembled metallo-supramolecular

*Corresponding author. Email: christopher.sumby@adelaide.edu.au

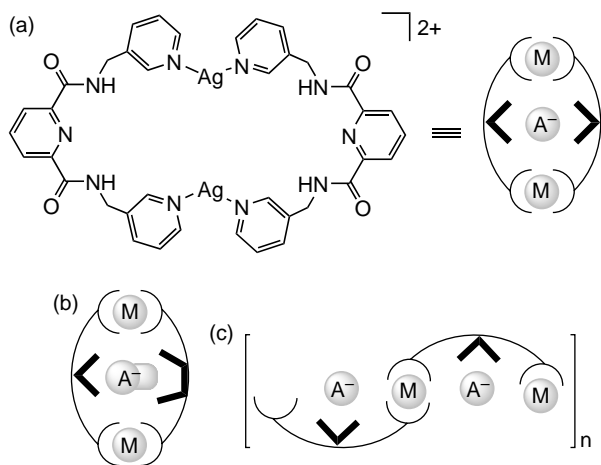


Figure 1. Schematic representations of the targeted metallo-supramolecular assemblies containing (a) one type of ligand or (b) a mixture of ligands. (c) An alternative, ring-opened coordination polymer form of structure (a).

species have been employed as anion sensors (39). In this latter context, we have directed our attention towards two major types of organic ligands, namely electron-deficient [3]radialene compounds (40–44) and heterocyclic amide ligands (45–47), in an effort to generate simple metallo-supramolecular assemblies and coordination polymers that encapsulate anions. Flexible bis-amide-containing ligands (Diagram 1) were chosen to probe the effects of having two different and potentially competing, orthogonal, supramolecular synthons in the same component, namely metal donor sites and hydrogen bond donor/acceptor moieties. Puddephatt has observed the effect of similar multiple supramolecular synthons in more rigid bis-amide compounds (48–51) and also for an isomer of **L1** (52). In two cases in the current work, **L4** and **L5**, the hydrogen bond donors are pre-organised to lessen the ability of the diamide compounds to form self-assembled hydrogen-bonded tapes (47).

Herein, we investigate the competing syntheses of discrete self-assembled metallo-macrocyclic compounds (Figure 1(a)) and coordination polymers (Figure 1(c)) of the diamide compounds **L1–L5** with silver(I) metal salts.

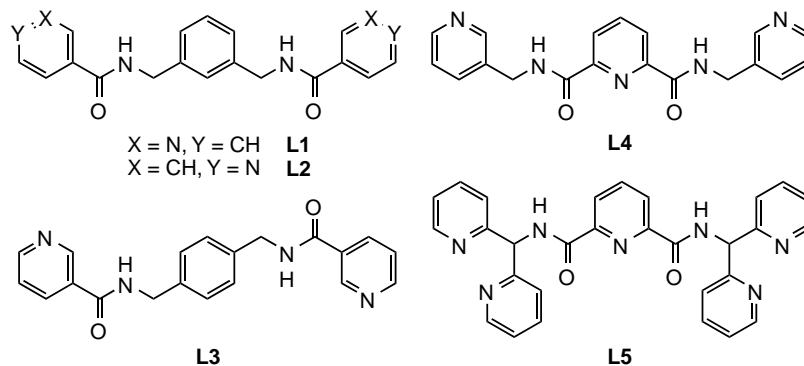


Diagram 1. The diamide ligands used in this study.

A new ligand **L5**, with chelating di-2-pyridylmethyl donor groups, was prepared. Three compounds were studied in solution by 1D and DOSY NMR spectroscopy and all were investigated by mass spectrometry, while X-ray crystallography was used to obtain the structures of three new metallo-macrocyclic complexes and three related coordination polymers. This enabled the consequences of competing supramolecular synthons to be investigated by comparing the solution and solid-state behaviour of each metal–ligand combination.

2. Experimental section

2.1 General experimental

Melting points were measured on a Gallenkamp melting point apparatus and are uncorrected. Elemental analyses were performed by the Campbell Microanalytical Laboratory at the University of Otago. Infrared spectra were collected on a PerkinElmer Spectrum BX FTIR spectrometer as KBr discs or on a PerkinElmer 100S FTIR spectrometer using a universal attenuated total reflectance (UATR) accessory. NMR spectra were recorded on a Varian Gemini 300 MHz or a Varian 600 MHz NMR spectrometer at 23°C using a 5 mm probe. ¹H NMR spectra recorded in CDCl₃ were referenced relative to the internal standard Me₄Si, while those recorded in DMSO-*d*₆ and CD₃CN were referenced to the solvent peak. Electrospray (ES) mass spectra were obtained using a Finnigan LCQ mass spectrometer. Unless otherwise stated, all chemicals were obtained from commercial sources and used as received. Dichloromethane was dried by standard literature procedures (53) and freshly distilled from calcium hydride. Compounds **L1–L4** were prepared according to the methods described in the literature (47).

2.2 Synthesis of 2,6-[*N,N'*-bis(di-(pyridin-2-yl)methyl)pyridine]-2,6-dicarboxamide hydrate (**L5** H₂O)

2,6-Pyridinedicarboxylic acid (1.06 g, 5.85 mmol) was suspended in dichloromethane (20 ml). Freshly distilled SOCl₂ (5 ml) and dry *N,N'*-dimethylformamide (DMF)

(100 μ l) were added and the reaction mixture was heated at reflux for 1 h. After cooling to room temperature, the solvent was removed *in vacuo* to give a white solid that was dried under high vacuum for 30 min. The solid was redissolved in CH_2Cl_2 (40 ml), di-(2-pyridyl)methylamine (0.58 g, 6.2 mmol) and NEt_3 (0.81 ml, 5.9 mmol) were added and the solution was heated at reflux for 24 h. The solvent was removed *in vacuo* to give a brown oil, and the residue was redissolved with dichloromethane (100 ml), washed with saturated sodium bicarbonate solution (2×100 ml) and chlorinated solvent layer dried over magnesium sulfate. The residue was purified by column chromatography, eluting with a methanol:dichloromethane (1:9) solvent system, to give **L5**· H_2O as an off-white solid (1.70 g, 51%). Mp 180–183°C. Anal found. C, 67.3; H, 4.7; N, 18.8. $\text{C}_{29}\text{H}_{25}\text{N}_7\text{O}_3$ requires C, 67.0; H, 4.9; N, 18.8%. ^1H NMR (300 MHz; CDCl_3 ; Me_4Si) δ 6.54 (2H, CH), 7.14 (4H, m, pyH5'), 7.60 (8H, m, pyH3', pyH4'), 8.02 (1H, t, pyH4), 8.37 (2H, d, pyH3 and pyH5), 8.50 (4H, 2d, pyH6') and 10.32 (2H, d, NH); (600 MHz; $\text{DMSO}-d_6$) δ 6.43 (2H, d, CH), 7.29 (4H, dd, pyH5'), 7.62 (4H, d, pyH3'), 7.78 (4H, t, pyH4'), 8.25 (3H, m, pyH3, pyH4, pyH5), 8.45 (4H, d, pyH6'), 8.50 (4H, 2d, pyH6') and 10.07 (2H, d, NH). ^{13}C (75.1 MHz; CDCl_3 ; Me_4Si) δ = 177.98, 149.57, 141.11, 137.19, 122.74, 122.31, 120.23, 103.87, 59.82. *m/z* (ES-MS) 501.6, (MH^+ , 15%), 523.4, (MNa^+ , 40%). Selected IR bands (KBr disc, cm^{-1}): 3378 (s), 3354 (s), 1724 (m), 1671 (s), 1587 (m), 1503 (s), 1436 (s) and 997 (s). Crystals of **L5** were obtained by slow evaporation of a methanol–acetonitrile solution.

2.3 Syntheses of Ag(I) compounds

2.3.1 $\{[\text{Ag}(\text{L1})(\text{CH}_3\text{CN})](\text{PF}_6)_n\}$ (6)

A solution of **L1** (35.6 mg, 0.103 mmol) in methanol (3 ml) was combined with an acetonitrile solution (1.5 ml) of AgPF_6 (25.9 mg, 0.102 mmol). Slow evaporation over a period of 2–3 weeks gave large colourless needles that had grown as clumps. The crystals were collected by filtration, washed with acetone and then with diethyl ether and dried under suction (30.0 mg, 46%). ^1H NMR (600 MHz, CD_3CN) δ 4.56, (d, 4H, CH_2), 7.25 (d, 2H, aryl H4 and H6), 7.31 (1H, t, aryl H5), 7.38 (1H, s, aryl H2), 7.47 (2H, dd, pyH5), 7.85 (bs, 2H, NH), 8.16 (2H, d, pyH4), 8.67 (2H, d, pyH6) and 8.96 (2H, s, pyH2). *m/z* (ES-MS, CH_3CN) 453.1 ($[\text{Ag}(\text{L1})]^+$, 67%), 455.1 ($[\text{Ag}(\text{L1})]^+$, 61%), 798.7 ($[\text{Ag}(\text{L1})_2]^+$, 100%), 800.7 ($[\text{Ag}(\text{L1})_2]^+$, 40%), 904.9 ($[\text{Ag}_2(\text{L1})_2]^+$, 5%), 906.9 ($[\text{Ag}^{109}\text{Ag}(\text{L1})_2]^+$, 8%), 908.8 ($[\text{Ag}^{109}\text{Ag}_2(\text{L1})_2]^+$, 5%), 1050.7 ($[\text{Ag}_2(\text{PF}_6)(\text{L1})_2]^+$, 24%), 1052.7 ($[\text{Ag}^{109}\text{Ag}(\text{PF}_6)(\text{L1})_2]^+$, 42%), 1054.7 ($[\text{Ag}_2(\text{PF}_6)(\text{L1})_2]^+$, 21%). Found: C, 41.4; H, 3.4; N, 10.8. $\text{C}_{22}\text{H}_{21}\text{N}_5\text{O}_2\text{F}_6\text{PAg}$ requires C, 41.3; H, 3.3; N, 10.9%. Selected IR bands (KBr disc, cm^{-1}): 3268 (s, N–H stretch), 3052, 2920 (m, C–H stretches),

2256 (w, $\text{C}\equiv\text{N}$ stretch), 1659 (s, $\text{C}=\text{O}$ stretch), 1629, 1592, 1543, 1352, 1298, 842 (s, P–F stretch), 709, 560.

2.3.2 $\{[\text{Ag}(\text{L2})(\text{NO}_3)\cdot(\text{H}_2\text{O})]\}_n$ (7)

A solution of **L2** (35.1 mg, 0.101 mmol) in warm methanol (4 ml) was combined with an acetonitrile solution (2 ml) of AgNO_3 (17.1 mg, 0.101 mmol). Slow evaporation over a period of 2–3 weeks gave large colourless blocks. The solution was decanted from the crystals, which were washed with acetone and then with diethyl ether and dried (25.5 mg, 49%). *m/z* (ES-MS, CH_3CN) 453.1 ($[\text{Ag}(\text{L2})]^+$, 73%), 455.1 ($[\text{Ag}(\text{L2})]^+$, 66%), 798.6 ($[\text{Ag}(\text{L2})_2]^+$, 75%), 800.6 ($[\text{Ag}(\text{L2})_2]^+$, 60%), 967.5 ($[\text{Ag}_2(\text{NO}_3)(\text{L2})_2]^+$, 6%), 969.6 ($[\text{Ag}^{107}\text{Ag}^{109}\text{Ag}(\text{NO}_3)(\text{L2})_2]^+$, 7%), 971.6 ($[\text{Ag}_2(\text{NO}_3)(\text{L2})_2]^+$, 5%). Found: C, 47.0; H, 3.6; N, 13.6. $\text{C}_{20}\text{H}_{18}\text{N}_5\text{O}_5\text{Ag}$ requires C, 46.5; H, 3.5; N, 13.6%. Selected IR bands (KBr disc, cm^{-1}): 3294 (s, N–H stretch), 3066, 2925 (m, C–H stretches), 1655 (s, $\text{C}=\text{O}$ stretch), 1611, 1549, 1425, 1383, 1315 (s, N–O stretches), 851, 693.

2.3.3 $\{[\text{Ag}_2(\text{CF}_3\text{CO}_2)_2(\text{L2})_2][\text{Ag}_2(\mu_2\text{-CF}_3\text{CO}_2)_2(\text{L2})_2]\}$ (8)

A methanol solution (4 ml) of **L2** (34.9 mg, 0.100 mmol) was combined with an acetonitrile solution (4 ml) of AgCF_3CO_2 (22.6 mg, 0.100 mmol). Slow evaporation over a period of 1 week gave large colourless blocks. The solution was decanted from the crystals, which were washed with acetone and then with diethyl ether and dried (42.4 mg, 75%). *m/z* (ES-MS, CH_3CN) 453.1 ($[\text{Ag}(\text{L2})]^+$, 69%), 455.1 ($[\text{Ag}(\text{L2})]^+$, 61%), 493.3 ($[\text{Ag}(\text{L2})(\text{CH}_3\text{CN})]^+$, 14%), 495.4 ($[\text{Ag}(\text{L2})(\text{CH}_3\text{CN})]^+$, 9%), 672.6 ($[\text{Ag}(\text{CF}_3\text{COO})(\text{L2} + \text{H}^+)]^+$, 18%), 674.6 ($[\text{Ag}(\text{CF}_3\text{COO})(\text{L2} + \text{H}^+)]^+$, 31%), 798.6 ($[\text{Ag}(\text{L2})_2]^+$, 70%), 800.6 ($[\text{Ag}(\text{L2})_2]^+$, 60%), 904.8 ($[\text{Ag}_2(\text{L2})_2]^+$, 5%), 906.8 ($[\text{Ag}^{107}\text{Ag}^{109}\text{Ag}(\text{L2})_2]^+$, 9%), 908.8 ($[\text{Ag}_2(\text{L2})_2]^+$, 5%), 1018.5 ($[\text{Ag}_2(\text{CF}_3\text{COO})(\text{L2})_2]^+$, 15%), 969.6 ($[\text{Ag}^{107}\text{Ag}^{109}\text{Ag}(\text{CF}_3\text{COO})(\text{L2})_2]^+$, 31%), 971.6 ($[\text{Ag}_2(\text{CF}_3\text{COO})(\text{L2})_2]^+$, 15%). Found: C, 46.9; H, 3.3; N 9.9. $\text{C}_{22}\text{H}_{18}\text{N}_4\text{O}_4\text{F}_3\text{Ag}$ requires C, 46.7; H, 3.2; N, 9.9%. Selected IR bands (UATR disc, cm^{-1}): 3307 (m, N–H stretch), 3074 (w, C–H stretch), 1738 (w, $\text{C}=\text{O}$ stretch), 1643 (s, $\text{C}=\text{O}$ stretch), 1541, 1421, 1184, 1127.

2.3.4 $\{[\text{AgNO}_3(\text{L3})\cdot(\text{CH}_3\text{OH})]\}_n$ (9)

A solution of **L3** (17.7 mg, 0.051 mmol) in methanol (3 ml) was combined with an acetonitrile solution (1 ml) of AgPF_6 (8.6 mg, 0.051 mmol). Slow evaporation over a period of 2–3 weeks gave colourless rods. The crystals of **9** were collected by filtration, washed with acetone and then with diethyl ether and dried under suction (11.0 mg, 39%). *m/z* (ES-MS, CH_3CN) 453.1 ($[\text{Ag}(\text{L3})]^+$, 100%), 455.1 ($[\text{Ag}(\text{L3})]^+$, 90%), 798.6 ($[\text{Ag}(\text{L3})_2]^+$, 86%), 800.6 ($[\text{Ag}(\text{L3})_2]^+$, 75%), 967.4 ($[\text{Ag}_2(\text{NO}_3)(\text{L3})_2]^+$, 7%),

969.6 ($[^{107}\text{Ag}^{109}\text{Ag}(\text{NO}_3)(\text{L3})_2]^+$, 9%), 971.6 ($[^{109}\text{Ag}_2(\text{NO}_3)(\text{L3})_2]^+$, 5%). Found: C, 46.4; H, 3.9; N 13.2. $\text{C}_{21}\text{H}_{22}\text{N}_5\text{O}_6\text{Ag}$ requires C, 46.0; H, 4.1; N 12.8%. Selected IR bands (KBr disc, cm^{-1}): 3355 (s, N—H stretch), 3062, 2948 (m, C—H stretches), 1635 (s, C=O stretch), 1593, 1540, 1384 (s, N—O stretch), 1300, 755, 703.

2.3.5 $[\text{Ag}_2(\text{NO}_2)_2(\text{L4})_2]$ (**10**)

A solution of **L4** (17.7 mg, 0.051 mmol) in methanol (2 ml) was combined with an acetonitrile solution (2 ml) of AgNO_2 (8.2 mg, 0.053 mmol). Slow evaporation over a period of 2–3 weeks gave colourless needles. The crystals were collected by filtration, washed with diethyl ether and dried under suction (19.5 mg, 76%). ^1H NMR (600 MHz, CD_3CN) δ 4.67, (d, 4H, CH_2), 7.36 (dd, 2H, $\text{pyH}5'$), 7.80 (2H, d, $\text{pyH}4'$), 8.11 (1H, t, $\text{pyH}4$), 8.21 (1H, d, $\text{pyH}3$ or $\text{pyH}5$), 8.29 (1H, d, $\text{pyH}3$ or $\text{pyH}5$), 8.43 (2H, d, $\text{pyH}6'$), 8.61 (2H, s, $\text{pyH}2'$) and 9.07 (2H, bs, NH). m/z (ES-MS, CH_3CN) 454.2 ($[^{107}\text{Ag}(\text{L4})]^+$, 95%), 456.1 ($[^{109}\text{Ag}(\text{L4})]^+$, 83%), 800.6 ($[^{107}\text{Ag}(\text{L4})_2]^+$, 100%), 802.7 ($[^{109}\text{Ag}(\text{L4})_2]^+$, 86%), 906.7 ($[^{107}\text{Ag}_2(\text{L4})(\text{L4}-\text{H})]^+$, 2%), 908.7 ($[^{107}\text{Ag}^{109}\text{Ag}(\text{L4})(\text{L4}-\text{H})]^+$, 4%), 910.8 ($[^{109}\text{Ag}_2(-\text{L4})(\text{L4}-\text{H})]^+$, 5%). Found: C, 45.7; H, 3.5; N, 16.8. $\text{C}_{38}\text{H}_{34}\text{N}_{12}\text{O}_8\text{Ag}_2$ requires C, 45.5; H, 3.4; N, 16.8%. Selected IR bands (UATR, cm^{-1}): 3345, 3267 (w, N—H stretches), 3047 (w, C—H stretch), 1673 (s, C=O stretch), 1530, 1207, 1189, 1166, 709.

2.3.6 $[\text{Ag}_2(\text{L5})_2](\text{NO}_3)_2 \cdot 2(\text{CH}_3\text{OH}) \cdot 2\text{H}_2\text{O}$ (**11**)

AgNO_3 (0.046 g, 0.27 mmol) was dissolved in methanol (5 ml), heated for a few minutes, before being added dropwise to a solution of **L5** (0.068 g, 0.135 mmol) which was dissolved in hot methanol–acetonitrile (15 ml). The resulting solution was heated for 45 min and left to evaporate at room temperature. After 1 month, the solution afforded $[\text{Ag}_2(\text{L5})_2](\text{NO}_3)_2$ as colourless rod-shaped crystals (20.0 mg, 21%). ^1H NMR (600 MHz, $\text{DMSO}-d_6$) δ 6.48 (2H, d, CH), 7.35 (4H, dd, $\text{pyH}5'$), 7.72 (4H, d, $\text{pyH}3'$), 7.85 (4H, t, $\text{pyH}4'$), 8.22 (3H, m, $\text{pyH}3$, $\text{pyH}4$, $\text{pyH}5$), 8.48 (4H, d, $\text{pyH}6'$), 8.50 (4H, 2d, $\text{pyH}6'$) and 10.01 (2H, d, NH). m/z (ES-MS, $\text{DMSO}/\text{methanol}$) 608.1 ($[^{107}\text{Ag}(\text{L5})]^+$, 100%), 610.1 ($[^{109}\text{Ag}(\text{L5})]^+$, 95%), 713.9 ($[^{107}\text{Ag}_2(\text{L5}-\text{H})]^+$, 9%), 715.9 ($[^{107}\text{Ag}^{109}\text{Ag}(\text{L5}-\text{H})]^+$, 18%), 717.9 ($[^{109}\text{Ag}_2(\text{L5}-\text{H})]^+$, 8%), 1214.6 ($[^{107}\text{Ag}_2(-\text{L5})(\text{L5}-\text{H})]^+$, 3%), 1216.8 ($[^{107}\text{Ag}^{109}\text{Ag}(\text{L5})(\text{L5}-\text{H})]^+$, 5%), 1218.8 ($[^{109}\text{Ag}_2(\text{L5})(\text{L5}-\text{H})]^+$, 3%). Selected IR bands (UATR, cm^{-1}): 3256 (w), 1654 (m), 1598 (m), 1527 (m), 1382 (s, N—O stretch), 1155 (m).

2.4 X-ray crystallography

In general, crystals were mounted under oil onto a plastic loop and X-ray data collected at low temperatures with $\text{Cu-K}\alpha$ ($\lambda = 1.5418 \text{ \AA}$, **L5**; Table 1) or $\text{Mo-K}\alpha$ radiation ($\lambda = 0.71073 \text{ \AA}$, **6–11**; Tables 1 and 2). Data were collected on (i) a Bruker Apex II CCD diffractometer or

Table 1. Crystal data and X-ray experimental data for **L5–L8**.

Compound	L5	L6	L7	L8
Empirical formula	$\text{C}_{29}\text{H}_{23}\text{N}_7\text{O}_2$	$\text{C}_{22}\text{H}_{21}\text{AgF}_6\text{N}_5\text{O}_2\text{P}$	$\text{C}_{20}\text{H}_{20}\text{AgN}_5\text{O}_6$	$\text{C}_{22}\text{H}_{18}\text{AgF}_3\text{N}_4\text{O}_4$
Formula weight	501.54	640.28	534.28	567.27
Temperature (K)	150(2)	89(2)	89(2)	89(2)
Crystal system	Monoclinic	Monoclinic	Orthorhombic	Monoclinic
Space group	$P2_1/c$	$P2_1/c$	$P2_12_12_1$	$C2/m$
a (Å)	11.0268(4)	9.5304(10)	8.0073(5)	16.128(3)
b (Å)	14.7568(5)	15.3420(19)	9.7288(5)	28.894(6)
c (Å)	15.3369(6)	16.846(2)	25.8930(16)	11.672(2)
β (°)	105.767(4)	99.527(6)		125.381(7)
Volume (Å ³)	2401.73(15)	2429.1(5)	2017.1(2)	4434.6(15)
Z	4	4	4	8
D_{calc} (mg/m ³)	1.387	1.751	1.759	1.699
Absorption coefficient (mm ⁻¹)	0.740	0.973	1.050	0.972
$F(000)$	1048	1280	1080	2272
Crystal size (mm ³)	0.24 × 0.15 × 0.06	0.45 × 0.09 × 0.06	0.18 × 0.16 × 0.05	0.68 × 0.40 × 0.05
Theta range for data (°)	9.51–71.33	1.81–27.00	2.24–32.32	1.41–27.67
Reflections collected	12,405	26,786	15,525	25,788
Independent reflections [$R(\text{int})$]	4526 [0.0430]	5298 [0.0279]	6824 [0.0347]	5136 [0.0282]
Completeness to theta max (%)	96.8	99.9	96.8	98.2
Observed reflections [$I > 2\sigma(I)$]	2792	4847	5820	4614
Data/restraints/parameters	4526/0/343	5298/1/352	6824/0/289	5136/0/415
Goodness of fit on F^2	0.784	1.042	1.026	1.134
R_1 [$I > 2\sigma(I)$]	0.0345	0.0349	0.0390	0.0440
wR_2 (all data)	0.0689	0.0853	0.0897	0.1286
Largest diff. peak and hole (e.Å ⁻³)	0.161 and -0.143	1.216 and -1.037	0.885 and -0.808	1.298 and -1.106
Absolute structure parameter			-0.04(2)	

Table 2. Crystal data and X-ray experimental data for **9**–**11**.

Compound	9	10	11
Empirical formula	C ₂₁ H ₂₂ AgN ₅ O ₆	C ₁₆ H ₁₇ AgN ₆ O ₄	C ₆₀ H ₅₈ Ag ₂ N ₁₆ O ₁₄
Formula weight	548.31	501.26	1442.96
Temperature (K)	89(2)	89(2)	150(2)
Crystal system	Triclinic	Triclinic	Orthorhombic
Space group	<i>P</i> – 1	<i>P</i> – 1	<i>Pbca</i>
<i>a</i> (Å)	9.2220(9)	8.0086(2)	10.0396(3)
<i>b</i> (Å)	9.5374(9)	9.3538(2)	23.0612(8)
<i>c</i> (Å)	13.5591(13)	13.5170(3)	25.4876(7)
α (°)	75.528(4)	100.812(1)	
β (°)	87.210(5)	100.476(1)	
γ (°)	67.492(4)	99.552(1)	
Volume (Å ³)	1065.30(18)	956.81(4)	5901.0(3)
<i>Z</i>	2	2	4
<i>D</i> _{calc} (mg/m ³)	1.709	1.740	1.624
Absorption coefficient (mm ⁻¹)	0.997	1.095	0.747
<i>F</i> (000)	556	504	2944
Crystal size (mm ³)	0.21 × 0.16 × 0.04	0.28 × 0.08 × 0.03	0.15 × 0.10 × 0.07
Theta range for data (°)	1.55–27.79	1.57–27.00	2.35–29.66
Reflections collected	21,188	16,659	29,891
Independent reflections [<i>R</i> (int)]	4906 [0.0424]	4168 [0.0255]	7666 [0.0553]
Completeness to theta max (%)	97.2	100.0	100.0
Observed reflections [<i>I</i> > 2 σ (<i>I</i>)]	4578	3871	4365
Data/restraints/parameters	4906/0/300	4168/0/271	7666/2/425
Goodness of fit on <i>F</i> ²	1.051	1.086	0.877
<i>R</i> ₁ [<i>I</i> > 2 σ (<i>I</i>)]	0.0446	0.0194	0.0394
<i>wR</i> ₂ (all data)	0.1367	0.0518	0.0772
Largest diff. peak and hole (e.Å ⁻³)	3.209 and –1.445	0.370 and –0.268	1.181 and –0.683

(ii) an Oxford Diffraction X-Calibur diffractometer. Data were corrected for polarisation and Lorentzian effects, and absorption corrections applied using a multi-scan method. Structures were solved by direct methods using SHELXS-97 (54) and refined by full-matrix least squares on *F*² by SHELXL-97 (55). Unless otherwise stated, all non-hydrogen atoms were refined anisotropically and hydrogen atoms were included as invariants at geometrically estimated positions. Diagrams were generated using the program X-Seed (56) as an interface to POV-Ray (57). Additional refinement details for individual structures are described below. CCDC numbers 873856–873862 contain the full crystal data for these structures. These data can be obtained from the Cambridge Crystallographic Data Centre via http://www.ccdc.cam.ac.uk/data_request/cif.

2.5 Additional refinement details

Compound 6: The hexafluorophosphate anion in **6** is disordered over two positions (77:23), and a DFIX restraint was used to maintain a sensible geometry for Part 2.

Compound 8: The pendant pyridyl rings of the two half-ligand moieties in the asymmetric unit are disordered over two positions (with approximately 50% occupancy). Both trifluoroacetate anions are disordered across mirror planes in the structure.

Compound 11: Two DFIX commands were used to maintain chemically sensible O–H bond lengths for the water solvate molecule.

3. Results and discussion

3.1 Ligand synthesis

Following the approach previously used to prepare related diamide ligands (47, 58, 59), di-(2-pyridyl)methylamine, which was synthesised in two steps using literature procedures (60–62), was reacted with 2,6-dimethylpyridine dichloride to give **L5** as a cream solid in *ca* 51% yield. Elemental analysis suggested that this product was obtained as the hydrate, **L5**·H₂O. This compound was characterised by ¹H NMR spectroscopy with the expected number of resonances for a symmetrical di-substituted derivative. The NH signal was observed significantly downfield at 10.32 ppm and the IR spectra of **L5** exhibit several characteristic strong bands, including a C=O stretching at approximately 1671 cm⁻¹, a strong band at 3354 cm⁻¹ that is attributed to the N–H stretching vibration, and a band at 1503 cm⁻¹ that is due to aromatic C=N stretches. ESI-MS, conducted in a mixture of methanol–acetonitrile solution, showed the expected positively charged ion of [**L5** + H]⁺ at *m/z* 501.6 (40%). Compound **L5** was recrystallised by dissolution in hot methanol–acetonitrile and on standing at room temperature for 5 days yielded colourless crystals

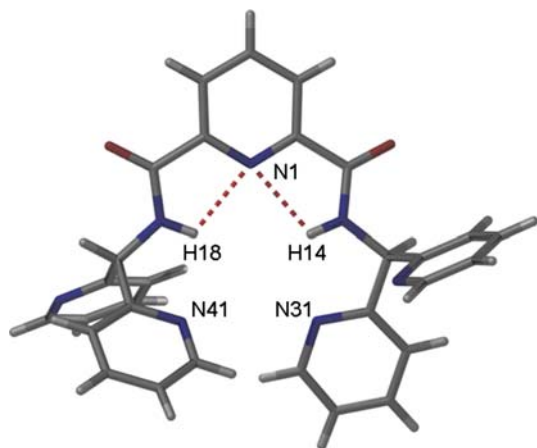


Figure 2. A view of the structure of compound **L5**. The weak pre-organising hydrogen bonds involving the 2,6-pyridine dicarboxamide core are shown but the hydrogen bonding involving the pendant pyridine rings is not shown.

with a plate morphology which were suitable for structure analysis using single crystal X-ray crystallography.

Compound **L5** crystallises in the monoclinic space group $P2_1/c$, with one complete molecule in the asymmetric unit. In the crystal structure, the two di-2-pyridylmethyl arms have quite different arrangements: one arm has the two 2-substituted pyridine rings directed either side of the plane of the 2,6-pyridine dicarboxamide core, while the second arm has one pyridine ring almost in the plane of the 2,6-pyridine dicarboxamide core and the other ring nearly perpendicular to the 2,6-pyridine dicarboxamide core. In the case of the second di-2-pyridylmethyl arm, the in-plane pyridine ring (N31) is involved in a weak hydrogen bond ($N-H\cdots N$: $d = 2.268 \text{ \AA}$, $D = 2.638 \text{ \AA}$, $\text{angle}_{\text{NHN}} = 105.14^\circ$) with one of the NH donors of the 2,6-pyridine dicarboxamide core. The other di-2-pyridylmethyl arm (N41) makes a similar weak electrostatic hydrogen bond with the other amide NH donor despite being twisted out of the plane. In a similar manner to the other diamide compounds investigated (47, 58, 59), the structure of compound **L5** demonstrates that the 2,6-pyridine dicarboxamide core pre-organises the amide moieties by weak intramolecular hydrogen bonding interactions ($N-H\cdots N$: $d = 2.241$ and 2.312 \AA , $D = 2.663$ and 2.699 \AA , $\text{angle}_{\text{NHN}} = 109.12^\circ$ and 109.65° ; Figure 2). In solution, the di-2-pyridylmethyl moieties are able to freely rotate about the C–N single bond to allow various coordination modes for **L5**. Aside from the intramolecular hydrogen bonding involving the pre-organised amide moiety and one of the pendant pyridine arms, the packing diagram does not reveal any other significant hydrogen bonding interactions.

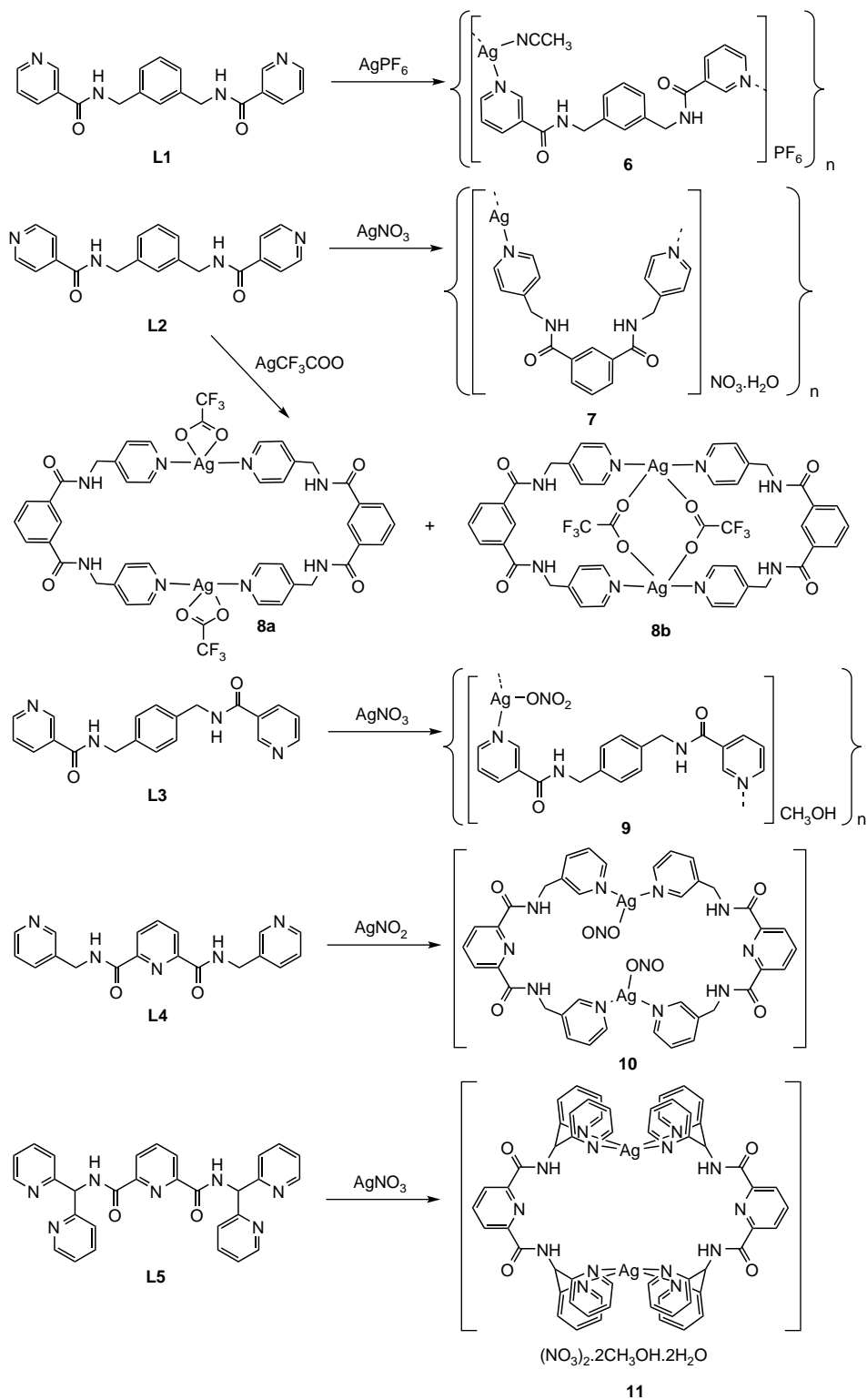
3.2 Coordination chemistry

Compounds **L1–L5** are all ditopic ligands that, under appropriate conditions, would be expected to form discrete metallo-macrocycles capable of encapsulating anions in the cavity formed within the macrocyclic structure. However, due to their inherent flexibility, it is also possible that coordination polymers may form. To understand the types of structures that can be obtained with compounds **L1–L5**, they were reacted with a range of silver salts (AgX where $X = \text{NO}_2, \text{NO}_3, \text{CF}_3\text{COO}$ and PF_6). This yielded crystalline samples of six silver complexes displaying either the desired discrete metallo-macrocyclic structures or 1D coordination polymers (Scheme 1), the latter of which are, in turn, assembled into 2D and 3D hydrogen-bonded networks. However, it was suspected that all compounds may form discrete structures in solution, and thus attempts were made to characterise all materials in solution by a combination of ^1H NMR spectroscopy, diffusion-ordered spectroscopy and mass spectrometry. In the solid state, all compounds were studied by IR spectroscopy, elemental analysis and single-crystal X-ray diffraction.

3.2.1 Synthesis of 1D coordination polymers

Reaction of AgPF_6 with **L1** in a mixture of acetonitrile and methanol followed by slow evaporation of the solvent mixture yielded colourless block-shaped crystals of $\{[\text{Ag}(\text{L1})(\text{CH}_3\text{CN})](\text{PF}_6)\}_n$ (**6**) in moderate 46% yield. In the solid state, the formulation of **6** was supported by elemental analysis and the observation of $\text{C}\equiv\text{N}$ triple bond stretch at 2256 cm^{-1} and a P–F stretch at 842 cm^{-1} . Similarly, a 1D coordination polymer of **L2**, $\{[\text{Ag}(\text{L2})(\text{NO}_3)(\text{H}_2\text{O})]\}_n$ (**7**), was also obtained by the reaction of this compound with AgNO_3 in 49% yield. This formulation for the bulk sample was confirmed by IR spectroscopy which revealed N–O stretches of the nitrate at 1383 cm^{-1} and a good match between the calculated and the found C, H and N values. Finally, reaction of **L3** with AgNO_3 gave another 1D coordination polymer, $\{[\text{Ag}(\text{L3})(\text{NO}_3)(\text{CH}_3\text{OH})]\}_n$ (**9**), which was also structurally characterised by X-ray crystallography. The IR spectrum revealed N–O stretches of the nitrate anion at 1384 cm^{-1} and N–H, C–H and C=O stretches consistent with the ligand at $3355, 2948$ and 1635 cm^{-1} , respectively.

To ascertain the behaviour of these compounds in solution, we investigated the ^1H and DOSY NMR spectroscopy and electrospray mass spectrometry (ES-MS) of all three compounds. ES-MS for **6** and **7** revealed molecular ions $[\text{Ag}_2(\text{X})(\text{L})_2]^+$ (where $\text{X} = \text{anion}$) that were consistent with the formation of either a [2 + 2] metallo-macrocycle or an oligomeric structure in solution. The corresponding molecular ions were not observed for compound **9**, as **L3** has a more divergent structure,

Scheme 1. The synthesis of discrete metallo-macrocycles and coordination polymers from **L1–L5**.

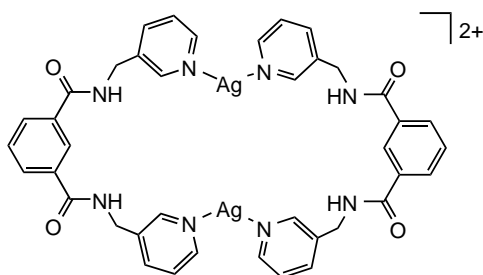


Diagram 2. A generic representation of a dinuclear metallo-macrocycle.

although peaks corresponding to $[\text{Ag}(\text{L}_2)]^+$ and $[\text{AgL}]^+$ were observed.

Compound **6** was soluble at suitable concentrations for NMR spectroscopy in CD_3CN , such solutions could be prepared by mixing appropriate ratios of AgPF_6 and **L1** or re-dissolving crystals of **6**. Limited coordination-induced shifts (CIS) were observed for this compound in CD_3CN , which combined with the number of chemical environments observed for the protons indicated that the product observed in solution was twofold symmetric. Despite the minimal CIS, DOSY revealed that the species present in solution had a diffusion coefficient of $4.95 \pm 0.05 \times 10^{-10} \text{ m}^2/\text{s}$; the diffusion coefficient of **L1** under the same conditions was $6.73 \pm 0.06 \times 10^{-10} \text{ m}^2/\text{s}$. As experimental diffusion rates obtained for two different spherical molecules in the same environment have been shown to be inversely proportional to the ratio of their radii (63–67), this indicates that the species formed from AgNO_3 and **L1** is larger than the original ligand. Such analysis has been utilised to estimate the relative size of a molecule from a comparison of the diffusion rates and is more readily applied than establishing a Stokes–Einstein relation for this type of system (68). The calculated ratio D_6/D_{L1} is 0.74, which is in agreement with the theoretical ratio of 0.72–0.75 expected for a dimeric structure (Diagram 2) (63–65, 68). Unfortunately, despite using both approaches to prepare NMR solutions, compounds **7** and **9** were not soluble in CD_3CN at suitable concentrations nor appear to be maintained in dimethylsulfoxide (DMSO) solution, and thus the corresponding analysis could not be completed.

Therefore, it appears that in solution compound **6** forms an $[\text{Ag}_2(\text{L1})_2]$ complex (Diagram 2) while it is unclear as to whether compounds **7** and **9** form oligomeric precursors to their solid-state structures or discrete metallo-macrocylic entities. Nonetheless, in the solid state, all three compounds form 1D coordination polymers that are self-assembled into 2D and 3D hydrogen-bonded networks. $\{[\text{Ag}(\text{L1})(\text{CH}_3\text{CN})](\text{PF}_6)\}_n$, compound **6**, crystallises in the monoclinic space group $P2_1/c$, with an asymmetric unit containing one molecule of **L1**, a silver atom, a coordinated acetonitrile solvent molecule and a hexafluorophosphate anion (with minor disorder of the equatorial fluorine atoms). The

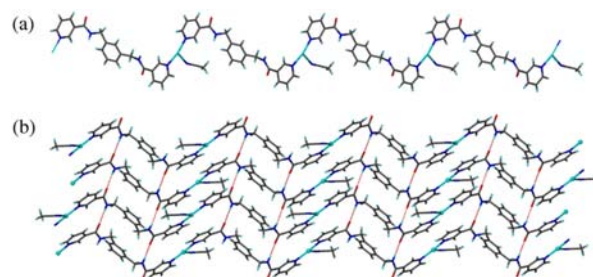


Figure 3. (a) A view of the 1D zigzag coordination polymer in the structure of $\{[\text{Ag}(\text{L1})(\text{CH}_3\text{CN})](\text{PF}_6)\}_n$. (b) The 2D hydrogen-bonded sheet formed from the 1D zigzag coordination polymer **6**. The 2D network lies in the *ab*-plane of the unit cell.

structure consists of a simple 1D zigzag coordination polymer that is hydrogen bonded to adjacent polymers through $\text{N}-\text{H} \cdots \text{O}=\text{C}$ hydrogen bonds. Unlike the *syn* or ‘U’-shaped structure of **L1** in the solid state (46), here **L1** adopts an alternate conformation in this structure and connects two T-shaped, but two-connecting silver cations ($\text{Ag}-\text{N}_{\text{py}}$ bond distances 2.167(2) and 2.178(2) Å; $\text{Ag}-\text{NCCH}_3$ distance 2.450(3) Å) to create a zigzag motif (Figure 3(a)). These 1D coordination polymers (which extend along the *b*-axis of the unit cell) are hydrogen bonded to adjacent polymers to create a hybrid coordination and hydrogen-bonded 2D network (Figure 3(b)) that has (4,4)-connectivity. The $\text{N}-\text{H} \cdots \text{O}=\text{C}$ amide hydrogen bonding interactions are typical ($\text{N}-\text{H} \cdots \text{O}$: $d = 2.011$ and 2.088 Å, $D = 2.857$ and 2.932 Å); thus, within the 2D network the ligand acts as a four-connecting centre. The self-complementary $\text{N}-\text{H} \cdots \text{O}=\text{C}$ amide hydrogen bonds are rigorously maintained in this structure, preventing any interactions with anionic (or otherwise) guests.

Crystals of $\{[\text{Ag}(\text{L2})](\text{NO}_3) \cdot (\text{H}_2\text{O})\}_n$ (**7**) were also obtained by slow evaporation, as colourless needles. The compound crystallises in the chiral orthorhombic space group $P2_12_12_1$, with one molecule of **L2**, a silver atom, a weakly coordinated nitrate anion and a solvate water molecule in the asymmetric unit. In this structure, the ligand adopts a ‘U’-shaped conformation not dissimilar to that observed in the solid state for **L2** (46). However, as observed in the structure of **L1**, the amide hydrogen bond donors are not directed into the cavity that is formed. Each molecule of the ligand coordinates to two silver atoms leading to the formation of a 1D coordination polymer. The polymeric structure is a helix (Figure 4(a)) that, when viewed down the helical axis (*b*-axis), has been contracted in one dimension and extended in the other (Figure 4(b)). The silver atoms have a linear geometry and are coordinated by two pyridyl donors (2.188(2) and 2.199(2) Å) of two different ligands; a nitrate makes a long contact with the silver atoms through a single oxygen atom (2.745(4) Å). A complete turn of the

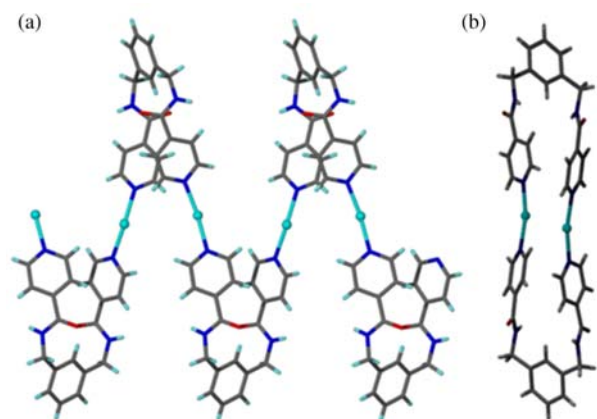


Figure 4. Two views of the helical 1D coordination polymer in the structure of **7**: (a) a side-on view of the helical polymer and (b) a representation looking down the helical axis.

helix, two repeating units of the polymer, equates to the length of the *b*-axis cell length of 9.73(1) Å.

In a similar manner to the structure of **6**, the amide functional groups of **L2** are involved in inter-polymer hydrogen bonding. Each helix is interdigitated by four other helices which form typical hydrogen bonds with one of the four amide functional groups in a repeating unit of the helix. Two views of this interdigitation are shown in Figure 5(a),(b). This bundling of the helices by hydrogen bonding leads to an apparently robust 3D M–L covalent and hydrogen-bonded network structure. Helical hydrogen-bonded chains of nitrate anions and water solvate molecules extend along the *b*-axis of the unit cell in the small channels, adjacent to the metal centre and between the coordination polymers (Figure 5(c)).

Complex $\{[\text{AgNO}_3(\text{L3})] \cdot (\text{CH}_3\text{OH})\}_n$ (**9**) crystallises in the triclinic space group *P* – 1 with one silver atom, one nitrate anion, a methanol solvate molecule and two half-molecules of the ligand in the asymmetric unit. The centroids of the ligands lie on centres of inversion. Each ligand coordinates two different T-shaped silver atoms, which in turn are coordinated by two ligand molecules to

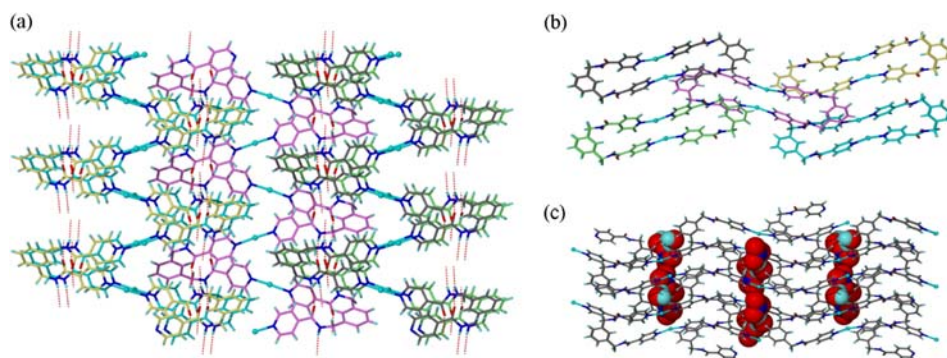


Figure 5. (a, b) Two views of the interdigitated bundles of helices in the structure of $\{[\text{Ag}(\text{L2})](\text{NO}_3) \cdot (\text{H}_2\text{O})\}_n$. (c) The helical hydrogen-bonded chains of nitrate anions and water solvate molecules in the channels of **7**.

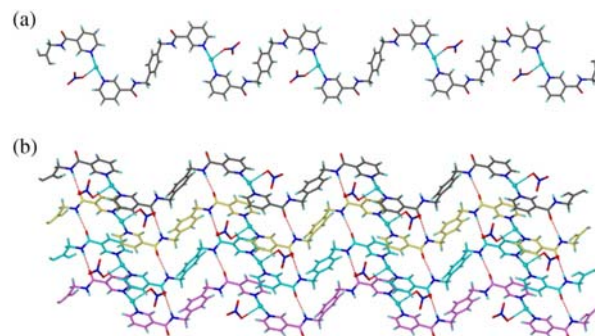


Figure 6. (a) A view of the 1D zigzag coordination polymer in the crystal structure of $\{[\text{AgNO}_3(\text{L3})] \cdot (\text{CH}_3\text{OH})\}_n$ (**9**). (b) The 2D hydrogen-bonded network in **9**. Individual chains are shown in different colours.

give a 1D coordination polymer (Figure 6(a)). The Ag–N distances are 2.159(3) and 2.164(3) Å, while the Ag–ONO₂ distance is comparatively longer at 2.681(4) Å. The 1D coordination polymer has a zigzag structure, akin to that observed for **L1** in the structure of **6**, where the nitrate anion coordinates in a similar manner to the acetonitrile solvate molecule in the previous structure. Despite **L3** having a *para*-substitution pattern in the central xylene ring, the Ag–Ag separation is shorter (16.00 Å) than observed in **6** where the xylene is *meta*-substituted.

Once again, the 1D coordination polymers are hydrogen bonded to give a 2D network structure (Figure 6(b)). Within the 2D network, the 1D coordination polymers are stacked almost directly on top of one another with the amide functionality twisted out of the plane of the coordination polymer. The hydrogen bonding distances between adjacent polymers are reasonably short (N–H···O: *d* = 1.994 and 2.073 Å, *D* = 2.774 and 2.889 Å). Each ligand molecule is hydrogen bonded to two other molecules of **L3** in adjacent coordination polymers and coordinated to two further molecules by the silver atoms. Thus, **L3** is a 4-connecting centre in this structure resulting in a (4,4)-connected network structure as observed for **6**. The packing within the crystal is completed by close packing of the 2D

networks with the coordinated nitrate anions in channels between the 2D layers. The methanol molecules, also located in these channels, are hydrogen bonded to an oxygen atom of an adjacent nitrate anion (O—H···O: $d = 2.024 \text{ \AA}$, $D = 2.834 \text{ \AA}$).

Despite forming a range of solution products, reaction of **L1**, **L2** and **L3** with silver(I) salts all form 1D coordination polymers that are self-assembled into 2D and 3D hydrogen-bonded networks in the solid state. It appears that in solution the competitive environment of the polar, hydrogen bond accepting solvents enables the formation of small oligomeric and metallo-macrocyclic structures, as confirmed in the case of **6**, yet as the solid-state structures form, ring opening of the metallo-macrocycles can occur to generate the 1D coordination polymers and to maximise the complementary hydrogen bonding between the orthogonal amide moieties. Such ring-opening polymerisation of metallo-macrocycles has been observed for other systems (42, 43, 48–52, 69, 70). In this case, the ring-opening polymerisation is favoured by the formation of complementary hydrogen-bonded tapes of the 1D coordination polymers.

3.2.2 Synthesis of the Ag(I) metallo-macrocycles

A second silver(I) complex (**8**) obtained with **L2** and AgCF_3COO in 75% yield has a rather complicated structure that consists of two related $[\text{Ag}_2(\text{L2})_2]$ metallo-macrocycles. In the solid state, the formulation of **8** was supported by elemental analysis and the observation of amide N—H stretch at 3307 cm^{-1} and an amide C=O stretch at 1643 cm^{-1} in the IR spectrum. Like coordination polymers **7** and **9**, compound **8** was not appreciably soluble in a single solvent and this prevented NMR studies from being conducted. The other two ligands investigated, **L4** and **L5**, possess one important difference over compounds **L1**–**L3**, specifically a central pyridine core that should pre-organise their conformation and favour the formation of discrete metallo-macrocycles in solution. This was initially confirmed in the solid state for both **L4** and **L5**. Reaction of **L4** with AgNO_2 gave crystals of a [2 + 2] metallo-macrocycle, $[\text{Ag}_2(\text{NO}_2)_2(\text{L4})_2]$ (**10**) in 76% yield. Similarly, reaction of **L5** with AgNO_3 gave colourless rod-like crystals of complex $[\text{Ag}_2(\text{L5})_2](\text{NO}_3)_2 \cdot 2\text{CH}_3\text{OH} \cdot 2\text{H}_2\text{O}$ (**11**) in 21% yield from slow evaporation of the methanol–acetonitrile reaction medium. The formation of compounds **10** and **11** was supported by elemental analysis and IR data confirming the presence of the ligands (C=O stretches: **10**, 1673 cm^{-1} ; **11**, 1654 cm^{-1}) and for **11**, nitrate anions with an N—O stretch at 1382 cm^{-1} .

The behaviour of the dinuclear metallo-macrocycles **10** and **11** in solution was investigated using ES-MS and NMR spectroscopy. The ES-MS of **10** revealed peaks for $[\text{Ag}_2(\text{L4})(\text{L4-H})]^+$ although these were in low relative abundance. In the ES-MS spectrum of compound **11**, dissolved in a mixture of DMSO and methanol, equivalent

molecular ions were observed that correspond to $[\text{Ag}_2(\text{L5})(\text{L5-H})]^+$. The ^1H NMR spectra of compounds **10** in CD_3CN and **11** in $\text{DMSO-}d_6$ indicated that the complexes remained intact in solution, with small CIS at the pyridyl protons being observed upon coordination to a silver atom.

Once again, despite the minimal CIS observed for **10** and **11**, DOSY was employed to examine the complexes in solution. In CD_3CN , **10** had a diffusion coefficient of $4.65 \pm 0.06 \times 10^{-10} \text{ m}^2/\text{s}$, while the diffusion coefficient of **L4** under the same conditions was $5.69 \pm 0.05 \times 10^{-10} \text{ m}^2/\text{s}$. The metallo-macrocyclic **10** has a very similar diffusion rate and thus size to the solution species **6** ($4.95 \pm 0.05 \times 10^{-10} \text{ m}^2/\text{s}$), although interestingly the diffusion rates for **L1** and **L4** differ more significantly. This perhaps points to the differing conformations of **L1** and **L4** in solution as comparing the calculated ratio of the diffusion rates of the complex versus the ligand, D_{10}/D_{L4} , gave a value of 0.82. This is a little outside the theoretical ratio of 0.72–0.75 expected for a dimeric structure (63–65, 68), perhaps as a consequence of the slower diffusion rate of **L4**, but still provides qualified support for the formation of a dinuclear metallo-macrocyclic. The theoretical ratios of the diffusion constants of 0.72–0.75 are calculated for hard sphere dimers, and thus will be lower than might be expected for metallo-macrocycles like the ones under consideration here. A comparison with the ratio of the radii (R) for **10** and **L4**, calculated from the volume of the species in their crystal structures, $R_{10}/R_{L4} = 0.76$, also provides a value lower than the ratio obtained experimentally from DOSY measurements. The corresponding analysis conducted for **11** in more viscous $\text{DMSO-}d_6$, the only common NMR solvent that **11** is soluble in, provided diffusion coefficients of $0.63 \pm 0.01 \times 10^{-10} \text{ m}^2/\text{s}$ for **11** and a diffusion coefficient under the same conditions of $0.75 \pm 0.03 \times 10^{-10} \text{ m}^2/\text{s}$ for **L5**. No direct comparison of the results obtained for **11** to those attained for **6** and **10** can be made as the measurements were undertaken in different solvents. However, the ratio of diffusion coefficients, D_{11}/D_{L5} was 0.84 and similar to the corresponding ratio for **10**, which provided evidence for maintenance of the solid-state structure in solution. The tightly packed nature of **11** (see Figure 10) means that the diffusion rate for this species may be faster than expected due to its smaller hydrodynamic volume, and thus the D_{11}/D_{L5} ratio is correspondingly higher.

The crystal structure of **8** is composed of two closely related [2 + 2] dimetallo-macrocyclic complexes, specifically $[\text{Ag}_2(\text{CF}_3\text{CO}_2)_2(\text{L2})_2]$ (**8a**) and $[\text{Ag}_2(\mu_2\text{-CF}_3\text{CO}_2)_2(\text{L2})_2]$ (**8b**) (Figure 7). The major difference between these two complexes is the presence of a trifluoroacetate anion that acts as a bidentate chelating ligand in one metallo-macrocyclic (**8a**) and a μ_2 -bridging ligand in the other (**8b**). The asymmetric unit consists of two independent half-ligand moieties, two silver atoms (both on a mirror plane) and two trifluoroacetate anions (also on a

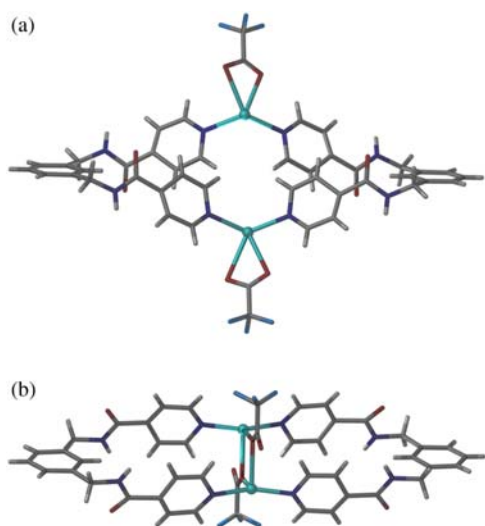


Figure 7. Perspective views of the metallo-macrocyclic based on (a) Ag1 (**8a**) and (b) Ag2 (**8b**) showing the distinct conformations observed in the solid state.

mirror plane). The pendant pyridyl rings of both half-ligand moieties are disordered. As a consequence of the different coordination mode of the trifluoroacetate anions, the silver atoms adopt slightly different coordination environments, albeit with the same mix of donors. Ag1 has a very distorted four coordinate geometry with a $131.95(16)^\circ$ angle between the pyridine donors and a Ag–N bond length of $2.262(3)$ Å. The Ag–O bond lengths to the chelating trifluoroacetate anions are $2.534(7)$ and $2.645(7)$ Å. In comparison, Ag2 has Ag–N bond lengths of $2.126(7)$ and $2.274(7)$ Å (for the disorder components) and Ag–O bond lengths of $2.530(4)$ and $2.544(4)$ for the bridging trifluoroacetate. The N–Ag–N angle is more linear for the macrocycle involving Ag2 with bond angles in the range $155.5(5)^\circ$ – $172.2(4)^\circ$, depending on the interpretation of the disorder model.

As a consequence of the two modes of trifluoroacetate coordination, the macrocycles have two quite different conformations. The Ag–Ag separations are $6.37(1)$ Å

(Ag1) and $3.66(1)$ Å (Ag2), and ligand conformations in the two metallo-macrocycles differ markedly. In the species involving Ag1, the ligand is severely twisted and while the Ag–Ag separation is larger, the silver atoms are actually pinched together but splayed apart in an orthogonal direction. Conversely, **L2** in the species involving Ag2 adopts a more typical conformation. The extent of the twisting can be seen by the comparison of the torsion angles for NH–CH₂–C1_{aryl}–C2_{aryl} about the central phenyl ring; in the first instance this twist is 29.1° where typically, and in the second macrocycle, it is 3.4° . No useful cavities are present in either metallo-macrocyclic, and as a consequence of the ligand conformation, the amide hydrogen bond donor/acceptor moieties are directed away from the metallo-macrocyclic core.

In the packing of the two metallo-macrocycles, there are weak Ag–Ag contacts (Ag–Ag distance 3.138 Å) that are well within the sum of the van der Waal's radii for silver(I) (71, 72). Due to the conformation of **L2**, both macrocycles form a number of hydrogen bonding interactions that generate a 3D hydrogen-bonded network. The formation of the 3D hydrogen-bonded network begins with the formation of hydrogen-bonded tapes of the two alternating metallo-macrocycles along the *c*-axis (Figure 8(a)). A total of eight intra-tape hydrogen bonds (N–H···O: $d = 2.090$ Å, $D = 2.941$ Å, angle_{NHO} 169.94° and C–H···O: $d = 2.202$ Å, $D = 3.122$ Å, angle_{CHO} 169.84°) connect each metallo-macrocyclic to two others. Each hydrogen-bonded tape is then bound to four other tapes through hydrogen bonds (Figure 8(b)). These inter-tape hydrogen bonds are relatively strong, N–H···O: $d = 1.862$ Å, $D = 2.693$ Å, angle_{NHO} 161.95° . This packing is reminiscent of the packing observed in compound **7**, whereby individual 1D coordination polymers are interdigitated with four others.

The metallo-macrocyclic formed from **L4** and AgNO₂ (**10**) adopts a comparatively simpler structure in the solid state. Crystallisation of **10**, as colourless crystals, was achieved by slow evaporation of an acetonitrile–methanol solution of the complex. Compound **10** crystallises in the

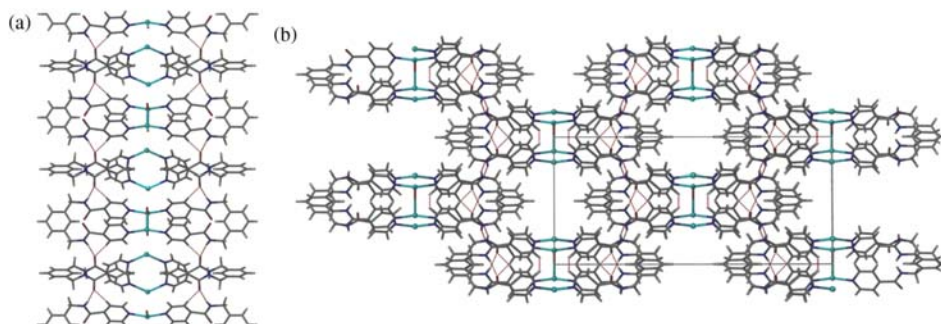


Figure 8. (a) A perspective view of the hydrogen-bonded tapes in **8**. (b) The crystal packing of **8** showing the inter-tape hydrogen bonding (in the *ab*-plane). The disorder components and the trifluoroacetate anions have been omitted for clarity; the void space observed in the figure is occupied predominantly by the anions.

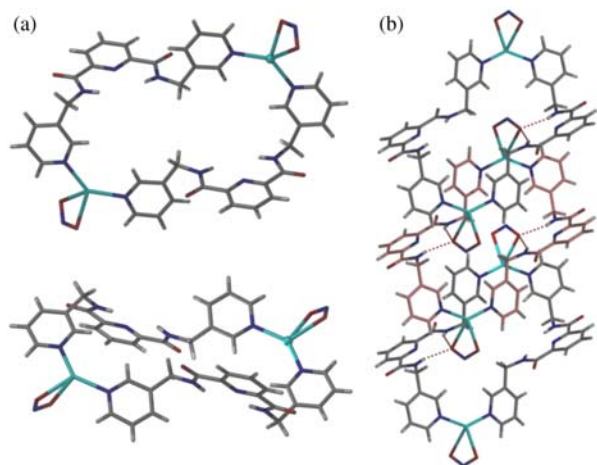


Figure 9. (a) Two perspective views of the $[\text{Ag}_2(\text{NO}_2)_2(\text{L4})_2]$ metallo-macrocycle **10**. (b) A view of the 1D hydrogen-bonded tapes in **10**.

triclinic space group $P - 1$ with a single molecule of **L4**, one silver atom and a coordinated nitrite anion in the asymmetric unit. The $[\text{Ag}_2(\text{NO}_2)_2(\text{L4})_2]$ metallo-macrocycle is generated by the operation of a centre of inversion (Figure 9). The silver centres are distorted tetrahedral with Ag–N bond lengths of 2.2209(14) and 2.2423(14) Å, and Ag–O bond lengths of 2.4547(13) and 2.604(1) Å. As shown in Figure 9(a), the metallo-macrocycle is far from planar and one 2,6-pyridine dicarboxamide unit is inclined up and the second down. The Ag–Ag separation within **10** is 13.36 Å.

Despite being pinched in the centre, the metallo-macrocycle is far more open than the structure of **8** and acts as a host for two coordinated nitrite anions of two adjacent molecules of **10**. Each nitrite anion forms two moderately strong hydrogen bonds with a 2,6-pyridine dicarboxamide unit ($\text{N}-\text{H}\cdots\text{O}$: $d = 2.192$ Å, $D = 2.990$ Å, $\text{angle}_{\text{NHO}} 154.37^\circ$ and $\text{N}-\text{H}\cdots\text{O}$: $d = 2.200$ Å, $D = 2.982$ Å, $\text{angle}_{\text{NHO}} 151.1^\circ$). These two hydrogen bonds are supported by several other weak hydrogen bonds involving the pyridyl hydrogens of **L4**. This results in the assembly of the molecules of **10** into hydrogen-bonded tapes (Figure 9(b)).

As noted, compound **11**, $[\text{Ag}_2(\text{L5})_2]$, is also a $[2 + 2]$ dimetallo-macrocyclic complex with **L5** acting as a bridging ligand. Compound **11** crystallises in the orthorhombic space group $Pbca$ with an asymmetric unit comprising one molecule of ligand **L5**, half of a silver atom, one non-coordinated nitrate, and non-coordinated water and methanol solvate molecules. A perspective view of **11** is shown in Figure 10 with the silver atoms in the structure coordinated by two ligand entities through the chelating pyridine donors, which results in a distorted tetrahedral geometry at each silver centre (bond angles in the range $82.20(8)^\circ - 140.29(8)^\circ$). The Ag–N bond lengths, in the range 2.315(2)–2.423(2) Å, are typical for tetrahedral silver(I) with four nitrogen heterocyclic donors.

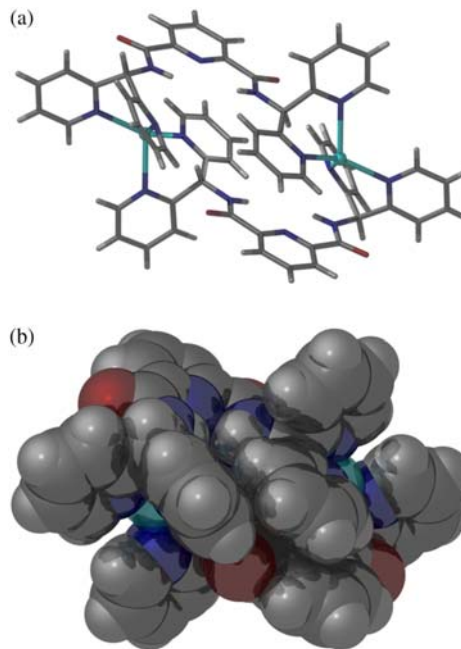


Figure 10. Two perspective views of the discrete metallo-macrocycle complex **11**.

In this dimer, the ligand acts as a bridge that provides a Ag–Ag distance of 8.170 Å. This complex has a similar structure to a discrete $[2 + 2]$ metallo-macrocylic silver complex incorporating 1,2-bis(di-2-pyridylaminomethyl)-benzene as a bridging ligand (**73**). Thus, it seems that the amide moieties do not play a significant role in favouring the formation of such entropically driven $[2 + 2]$ assemblies. However, it is worth noting that the previously reported complex has a more open metallo-macrocylic structure compared with complex **11** and is stabilised by Ag– π interactions. No such interactions are observed in this complex as the pyridyl donors saturate the coordination requirements of the metal centres. Although the amide NH donors point into the centre of the complex, the resulting cavity is too small for guest inclusion and, due to the steric bulk of the ligand, not accessible (Figure 10(b)). Due to this internalisation of the hydrogen bond donors in the crystal packing, no significant hydrogen bond interactions between the complex and the solvents or anion were identified.

In contrast to the preferential formation of coordination polymers by ligands **L1**–**L3** in the solid state, notwithstanding the result obtained for complex **8**, **L4** and **L5** appear to favour the formation of discrete metallo-macrocylics both in solution and in the solid state. This facility is a consequence of the pre-organising effect of the 2,6-pyridine dicarboxamide moiety as noted by others (**74**, **75**), but presumably also the resulting hydrogen bond donor–acceptor mismatch that occurs by having one hydrogen bond donor region and two separate hydrogen bond acceptor carbonyl moieties. This disfavors the

formation of hydrogen-bonded tapes or networks that support the crystal packing in the structures of the coordination polymers encountered with **L1**–**L3**. The effect of pre-organisation was previously observed in solid-state structures of **L1**–**L4** alone (47).

4. Conclusion

In this work, we have examined the self-assembly of five flexible heterocyclic diamide ligands with silver(I) metal salts with the intention of forming discrete metallo-supramolecular structures with anion-complexing ability. From this work, the structures of three new metallo-macrocylic complexes and three related coordination polymers were obtained. It was observed that compounds **L1**–**L3**, which lack the pre-organising effect of a central 2,6-pyridine dicarboxamide core, appear to preferentially form 1D coordination polymers, {[Ag(**L1**)(CH₃CN)](PF₆)}_n (**6**), {[Ag(**L2**)](NO₃·(H₂O))}_n (**7**) and {[AgNO₃(**L3**)]·(CH₃OH)}_n (**9**), which in turn form 2D and 3D hydrogen-bonded networks stabilised through orthogonal hydrogen bonding interactions. This precludes the formation of the desired hydrogen bond donor pockets to selectively complex anions. This is despite the observation that at least one system, **L1**, appears to form a discrete metallo-macrocylic structure in solution. Thus, in solution, where solvent molecules are capable of acting as hydrogen bond acceptors, discrete structures for **L1**–**L3** can be obtained. This contrasts with the behaviour encountered for the structurally similar diamide ligand **L4** that possess the pre-organising central 2,6-pyridine dicarboxamide core; the structure of [Ag₂(NO₂)₂(**L4**)₂] (**10**) in solution and in the solid state is a dinuclear metallo-macrocylic. This was confirmed by ES-MS and DOSY NMR spectroscopy in solution and X-ray crystallography in the solid state. A fifth ligand, **L5**, with two chelating di-2-pyridylmethyl donor groups, was also prepared to further favour discrete metallo-macrocylic species in solution. The resulting silver(I) complex, [Ag₂(**L5**)₂](NO₃)₂·2CH₃OH·2H₂O (**11**), forms such a structure in solution and in the solid state but unfortunately lacks any internal cavity due to its steric bulk. In one instance, **L2** gives rise to a dinuclear metallo-macrocylic that in the solid state exists as supramolecular isomers, namely [Ag₂(CF₃CO₂)₂(**L2**)₂] and [Ag₂(μ₂-CF₃CO₂)₂(**L2**)₂].

This study has further demonstrated the effect of competing supramolecular synthons, covalent M–L bonding and hydrogen bonding, on the self-assembly of discrete metallo-supramolecular systems containing flexible diamide ligands. The dichotomy of structures appears to be a consequence of having very similarly matched driving forces for hydrogen bonding interactions versus covalent M–L bonding for these materials. In pursuit of our ambitions of self-assembling metallo-supramolecular species capable of responsive binding of anions, we are

currently looking at several approaches to limit the propensity of these compounds to form the hydrogen-bonded networks observed in **6**, **7** and **9**. These include continuing to utilise pre-organised binding pockets (like **L4**) and synthesising the thioamide analogues of **L1**–**L3**.

Acknowledgements

C.J.S. thanks the Australian Research Council for an Australian Post-doctoral Fellowship and a Future Fellowship (FT0991910), and supporting this research through a Discovery Project (DP0773011). M.A.K. thanks the Ministry of Higher Education, Malaysia, and the University Malaysia Terengganu for financial support. The University of Otago is acknowledged for providing access to facilities for X-ray crystallography.

Note

1. Current address: Department of Chemical Sciences, Faculty of Science and Technology, University Malaysia Terengganu, 21030 Terengganu, Malaysia.

References

- (1) Pluth, M.D.; Raymond, K.N. *Chem. Soc. Rev.* **2007**, *36*, 161–171.
- (2) Glasson, R.K.; Lindoy, L.F.; Meehan, G.V. *Coord. Chem. Rev.* **2008**, *252*, 940–963.
- (3) Yoshizawa, M.; Klosterman, J.K.; Fujita, M. *Angew. Chem. Int. Ed.* **2009**, *48*, 3418–3438.
- (4) Pluth, M.D.; Bergman, R.G.; Raymond, K.N. *Acc. Chem. Res.* **2009**, *42*, 1650–1659.
- (5) Mercer, D.J.; Loeb, S.J. *Chem. Soc. Rev.* **2010**, *39*, 3612–3620.
- (6) Inokuma, Y.; Kawano, M.; Fujita, M. *Nat. Chem.* **2011**, *3*, 349–358.
- (7) Begum, R.A.; Kang, S.O.; Day, V.W.; Bowman-James, K. In *Anion Coordination Chemistry*; Bowman-James, K., Bianchi, A., Garcia-Espana, E., Eds.; Wiley-VCH Verlag & Co. KGaA, Weinheim, Germany, 2012; p 141–225.
- (8) Bianchi, A.; Garcia-Espana, E. In *Anion Coordination Chemistry*; Bowman-James, K., Bianchi, A., Garcia-Espana, E., Eds.; Wiley-VCH Verlag and Co. KGaA, Weinheim, Germany, 2012; p 75–140.
- (9) Kang, S.-O.; Linares, J.M.; Day, V.W.; Bowman-James, K. *Chem. Soc. Rev.* **2010**, *39*, 3980–4003.
- (10) Bates, G.W.; Gale, P.A. *Struct. Bond.* **2008**, *129*, 1–44.
- (11) Beer, P.D.; Gale, P.A. *Angew. Chem. Int. Ed.* **2001**, *40*, 486–516.
- (12) Kang, S.O.; Begum, R.A.; Bowman-James, K. *Angew. Chem. Int. Ed.* **2006**, *45*, 7882–7894.
- (13) Bowman-James, K. *Acc. Chem. Res.* **2005**, *38*, 671–678.
- (14) Hay, B.P.; Bryantsev, V.S. *Chem. Commun.* **2008**, 2417–2428.
- (15) Schottel, B.L.; Chifotides, H.T.; Dunbar, K.R. *Chem. Soc. Rev.* **2008**, *37*, 68–83.
- (16) Hay, B.P.; Custelcean, R. *Cryst. Growth Des.* **2009**, *9*, 2539–2545.
- (17) Frontera, A.; Gamez, P.; Mascal, M.; Mooibroek, T.J.; Reedijk, J. *Angew. Chem. Int. Ed.* **2011**, *50*, 9564–9583.
- (18) Yoon, J.; Kim, S.K.; Singh, N.J.; Kim, K.S. *Chem. Soc. Rev.* **2006**, *35*, 355–360.
- (19) Vilar, R. *Angew. Chem. Int. Ed.* **2003**, *42*, 1460–1477.
- (20) Vilar, R. *Struct. Bond.* **2008**, *129*, 175–206.

- (21) Vilar, R. *Eur. J. Inorg. Chem.* **2008**, 357–367.
- (22) Rice, C.R. *Coord. Chem. Rev.* **2006**, 250, 3190–3199.
- (23) Custelcean, R. *Chem. Soc. Rev.* **2010**, 39, 3675–3685.
- (24) Custelcean, R.; Moyer, B.A. *Eur. J. Inorg. Chem.* **2007**, 1321–1340.
- (25) Applegarth, L.; Goeta, A.E.; Steed, J.W. *Chem. Commun.* **2005**, 2405–2406.
- (26) Steed, J.W. *Chem. Commun.* **2006**, 2637–2649.
- (27) Leong, W.L.; Vittal, J.J. *Chem. Rev.* **2011**, 111, 688–764.
- (28) Rajput, L.; Biradha, K. *New J. Chem.* **2010**, 34, 2415–2428.
- (29) Janiak, C.; Vieth, J.K. *New J. Chem.* **2010**, 34, 2366–2388.
- (30) Adarsh, N.N.; Kumar, D.K.; Suresh, E.; Dastidar, P. *Inorg. Chim. Acta* **2010**, 363, 1367–1376.
- (31) Aakeroy, C.B.; Champness, N.R.; Janiak, C. *CrystEngComm* **2010**, 12, 22–43.
- (32) Beer, P.D. *Acc. Chem. Res.* **1998**, 31, 71–80.
- (33) O’Neil, E.J.; Smith, B.D. *Coord. Chem. Rev.* **2006**, 250, 3068–3080.
- (34) Qin, Z.; Jennings, M.C.; Puddephatt, R.J. *Inorg. Chem.* **2003**, 42, 1956–1965.
- (35) Yue, N.L.S.; Eisler, D.J.; Jennings, M.C.; Puddephatt, R.J. *Inorg. Chem.* **2004**, 43, 7671–7681.
- (36) Goetz, S.; Kruger, P.E. *Dalton Trans.* **2006**, 1277–1284.
- (37) Diaz, P.; Tovilla, J.A.; Ballester, P.; Benet-Buchholz, J.; Vilar, R. *Dalton Trans.* **2007**, 3516–3525.
- (38) Tovilla, J.A.; Carlqvist, P.; Benet-Buchholz, J.; Maseras, F.; Vilar, R. *Supramol. Chem.* **2007**, 19, 599–611.
- (39) Mishra, A.; Vajpayee, V.; Kim, H.; Lee, M.H.; Jung, H.; Wang, M.; Stang, P.J.; Chi, K.-W. *Dalton Trans.* **2012**, 41, 1195–1201.
- (40) Avellaneda, A.; Hollis, C.A.; He, X.; Sumbly, C.J.; Beilstein *J. Org. Chem.* **2012**, 8, 71–80.
- (41) Hollis, C.A.; Hanton, L.R.; Morris, J.C.; Sumbly, C.J. *Cryst. Growth Des.* **2009**, 9, 2911–2916.
- (42) Steel, P.J.; Sumbly, C.J. *Chem. Commun.* **2002**, 322–323.
- (43) Steel, P.J.; Sumbly, C.J. *Inorg. Chem. Commun.* **2002**, 5, 323–327.
- (44) Evans, J.D.; Hollis, C.A.; Hack, S.; Hoffmann, P.; Gentleman, A.S.; Buntine, M.A.; Sumbly, C.J.; submitted.
- (45) Abdul-Kadir, M.; Hanton, L.R.; Sumbly, C.J. *Dalton Trans.* **2012**, 41, 4497–4505.
- (46) Abdul-Kadir, M.; Hanton, L.R.; Sumbly, C.J. *Dalton Trans.* **2011**, 40, 12374–12380.
- (47) Sumbly, C.J.; Hanton, L.R. *Tetrahedron* **2009**, 65, 4681–4691.
- (48) Yue, N.L.S.; Jennings, M.C.; Puddephatt, R.J. *Eur. J. Inorg. Chem.* **2007**, 1690–1697.
- (49) Yue, N.L.S.; Jennings, M.C.; Puddephatt, R.J. *Dalton Trans.* **2006**, 3886–3893.
- (50) Yue, N.L.S.; Jennings, M.C.; Puddephatt, R.J. *Inorg. Chem.* **2005**, 44, 1125–1131.
- (51) Yue, N.L.S.; Jennings, M.C.; Puddephatt, R.J. *Chem. Commun.* **2005**, 4792–4794.
- (52) Yue, N.L.S.; Jennings, M.C.; Puddephatt, R.J. *Dalton Trans.* **2010**, 39, 1273–1281.
- (53) Amargo, L.F.W.; Chai, L.L.C. *Purification of Laboratory Chemicals*; 5th Ed. Elsevier Butterworth-Heinemann, Oxford, United Kingdom, 2003.
- (54) Sheldrick, G.M. *Acta Crystallogr.* **1990**, A46, 467–473.
- (55) Sheldrick, G.M. *SHELXL-97*; University of Göttingen: Göttingen, 1997.
- (56) Barbour, L.J. *J. Supramol. Chem.* **2001**, 1, 189–191.
- (57) Persistence of Vision Raytracer Pty. Ltd, *POV-Ray*; Williamstown, Australia, 2003.
- (58) Napatupulu, M.; Griggs, B.L.; Luo, S.-X.; Turner, P.; Maeder, M.; Lawrance, G.A. *J. Heterocycl. Chem.* **2009**, 46, 243–250.
- (59) Napatupulu, M.; Lawrance, G.A.; Clarkson, G.J.; Moore, P. *Aust. J. Chem.* **2006**, 59, 796–804.
- (60) Renz, M.; Hemmert, C.; Meunier, B. *Eur. J. Org. Chem.* **1998**, 1271–1273.
- (61) David, B.; Jin, C.; Plummer, S.; Berman, E.S.F.; Striplin, D. *Inorg. Chem.* **2004**, 43, 1735–1742.
- (62) Blicke, F.F.; Maxwell, C.E. *J. Am. Chem. Soc.* **1939**, 61, 1780–1782.
- (63) Krishnan, V.V. *J. Magn. Reson.* **1997**, 124, 468–473.
- (64) Cameron, K.S.; Fielding, L. *J. Org. Chem.* **2001**, 66, 6891–6895.
- (65) Kotch, F.W.; Sidorov, V.; Lam, Y.-F.; Kayser, K.J.; Li, H.; Kaucher, M.S.; Davis, J.T. *J. Am. Chem. Soc.* **2003**, 125, 15140–15150.
- (66) Megyes, T.; Jude, H.; Grósz, T.; Bakó, I.; Radnai, T.; Tárkányi, G.; Pálkás, G.; Stang, P.J. *J. Am. Chem. Soc.* **2005**, 127, 10731–10738.
- (67) Floquet, S.; Brun, S.; Lemonnier, J.-F.; Henry, M.; Delsuc, M.-A.; Prigent, Y.; Cadot, E.; Taulelle, F. *J. Am. Chem. Soc.* **2009**, 131, 17254–17259.
- (68) Sumbly, C.J.; Fisher, J.; Prior, T.J.; Hardie, M.J. *Chem. Eur. J.* **2006**, 12, 2945–2959.
- (69) Lozano, E.; Nieuwenhuyzen, M.; James, S.L. *Chem. Eur. J.* **2001**, 7, 2644–2651.
- (70) James, S.L. *Chem. Soc. Rev.* **2009**, 38, 1744–1758.
- (71) Bondi, A. *J. Phys. Chem.* **1964**, 68, 441–451.
- (72) Singh, K.; Long, J.R.; Stavropoulos, P. *J. Am. Chem. Soc.* **1997**, 119, 2942–2943.
- (73) Antonioli, B.; Bray, D.J.; Clegg, J.K.; Glöe, K.; Glöe, K.; Kataeva, O.; Lindoy, L.F.; McMurtrie, J.C.; Sumbly, C.J.; Steel, P.J.; Wenzel, M. *Dalton Trans.* **2006**, 4783–4794.
- (74) Berl, V.; Huc, I.; Khoury, R.G.; Lehn, J.-M. *Chem. Eur. J.* **2001**, 7, 2798–2809.
- (75) Choi, K.; Hamilton, A.D. *Coord. Chem. Rev.* **2003**, 240, 101–110.